Available online at www.sciencedirect.com
ScienceDirect
Journal of the European Ceramic Society 29 (2009) 2589–2594
www.elsevier.com/locate/jeurceramsoc

# Crystal structure and orthorhombic–tetragonal phase transition of nanoscale $(Li_{0.06}Na_{0.47}K_{0.47})NbO_3$

Chao Wang, Yu-Dong Hou *, Hai-Yan Ge, Man-Kang Zhu, Hui Yan

*Key Laboratory of Advanced Functional Materials of China Education Ministry, College of Materials Science and Engineering, Beijing University of Technology, Beijing 100124, People's Republic of China*

Received 30 December 2008; received in revised form 11 February 2009; accepted 19 February 2009
Available online 19 March 2009

**Abstract**

Lead-free nano $(Li_{0.06}Na_{0.47}K_{0.47})NbO_3$ powders, with pure perovskite structure and various grain sizes between about 30 and 60 nm, have been successfully synthesized by a novel sol–gel method, in which $Nb_2O_5$ was used as the Nb source. The refining XRD and Raman spectra were used in combination with TEM to investigate the evolution of lattice structure and phase transformation behavior as a function of grain size. The results demonstrated that the growth process of grains has been divided into two stages, and the distortion of unit cell apparently decreases with decreasing grain size. At around 35 nm, the phase structure of $(Li_{0.06}Na_{0.47}K_{0.47})NbO_3$ changed from orthorhombic to tetragonal. This phenomenon is related to a grain size-induced structural phase transition. For the well accepted wisdom that niobates get super piezoelectric properties in orthorhombic–tetragonal transition region, our results suggested a critical size for the application of $(Li_{0.06}Na_{0.47}K_{0.47})NbO_3$ in nano piezoelectric devices.


*Keywords:* Sol–gel processes; Niobates; Nanocomposites; Grain size; Orthorhombic–tetragonal phase transition

## 1. Introduction

(Na, K)$NbO_3$ (NKN) based ceramics have attracted much attention recently as they represent an environmentally friendly alternative to compositions based on heavy metals, such as Pb(Zr,Ti)$O_3$ (PZT). It is believed that in PZT ceramics, morphotropic phase boundary (MPB), which is nearly vertical in the temperature-composition phase diagram,[1,2] plays a very important role because piezoelectric and dielectric properties show a maximum around the MPB. However, the so-called MPB in NKN based ceramics is very different from that in PZT based ceramics. It is actually an orthorhombic–tetragonal (O–T) polymorphic phase transition (PPT) and shows strong temperature dependence.[3] Generally, the large number of thermodynamically equivalent states near the PPT allows a high degree of alignment of ferroelectric dipoles, which result in a dramatic enhancement in the electrical properties of NKN based ceramic. For the reason that PPT is temperature dependent, many recent studies concern about designing different composites to turn the O–T phase transition from about 200 °C to room temperature.[4,5] Of all the NKN based ceramics, $(Li_{0.06}Na_{0.47}K_{0.47})NbO_3$ (LNKN) is one of the most intensively studied system due to the PPT structure near room temperature. The LNKN ceramics show the large piezoelectric constant $d_{33}$ over 200 pC/N, and are considered as a new generation materials for lead-free piezoelectric devices.[6–8] On the other hand, continuous advances in microelectronics are leading to the miniaturization of piezoelectric components; therefore, the fundamental investigation of properties of nanoscale LNKN become very important due to their potential application in nanoscale devices and a known difference in behavior relative their bulk counterparts. It is well known that the crystal symmetry increases with decreasing grain sizes.[9,10] This phenomenon, which is called "size effect", could cause problems for future miniaturization of piezoelectric components, and size effect on many systems, such as $BaTiO_3$, $(Pb_{0.9}La_{0.1})TiO_3$, and so on, has been intensively studied.[11–13] It is to say, except chemistry composite, grain size could also influence the O–T phase transition of NKN based materials, and which is rarely studied. Therefore, the research of size effect on nanoscale LNKN is one of the

* Corresponding author. Tel.: +86 10 67392445; fax: +86 10 67392445.
*E-mail address:* ydhou@bjut.edu.cn (Y.-D. Hou).

0955-2219/$ – see front matter © 2009 Elsevier Ltd. All rights reserved.
doi:10.1016/j.jeurceramsoc.2009.02.012

most important assignments from the scientific and industrial viewpoints.

Sol–gel process has attracted much attention in materials synthesis due to the ease of tuning material composition through the use of molecular precursors. The metal organic complexes mix and react on a molecular-scale favoring a homogeneous product composition.[14–16] Moreover, powders with different grain size could be facilely prepared by the sol–gel process using different calcination temperatures, which favored to the study of size effect of ferroelectric powders. In this study, a newly developed sol–gel route has been used to prepare LNKN nanoscale system. The growth process of nanoscale LNKN and grain size-induced O–T phase transition have been studied, and the mechanism of grain size-induced structural phase transformation has been discussed.

## 2. Experimental

$Nb_2O_5$ (99.9%), KOH (97%), $Li_2CO_3$ (97%), $Na_2CO_3$ (99.8%), $K_2CO_3$ (99%), acetic acid ($CH_3COOH$, 99.5%), oxalic acid ($(COOH)_2{\cdot}2H_2O$, 99.5%), citric acid ($C_6H_8O_7{\cdot}H_2O$, 99.5%), $HNO_3$ (65.0–68.0%), and $NH_3{\cdot}H_2O$ (25.0–28.0%) were used as raw materials. The LNKN gels were synthesized by a novel sol–gel method,[17] in which $Nb_2O_5$ was changed into a water-soluble species through the chemical chelation as the Nb source. In order to obtain nano powders with different grain sizes, the calcination temperatures of gels were precisely controlled from 400 to 650 °C.

The crystal phase of the powders was determined using X-ray diffractometry (XRD; Model D8 Advance, Bruker AXS, Karlsruhe, Germany) in $\theta$–$2\theta$ mode with graphite monochromatized Cu K$\alpha$ radiation ($\lambda = 0.154178$ nm). The scan step was 0.005° and the scan speed was 0.3 s/step in the ranges of 20°–60°. The average grain size was calculated from the full width at half maximum (FWHM) of the diffraction lines by using Topas 2P software according to Scherrer's relation[18]:

$$d = \frac{K\lambda}{B\cos\theta} \quad (1)$$

where $d$ is the grain diameter, $\lambda$ the X-ray wavelength, $\theta$ the diffraction angle, $B$ the FWHM of the diffraction peak, and $K$ the Scherrer constant. In addition, the microstrain of the particles was also refined by using Topas 2P software. To reduce errors, all diffraction peaks between 20° and 60° were used to calculate the average grain size and microstrain. The powder morphology was observed by a transmission electron microscopy (TEM; Model JEM-2000 F, JEOL, Tokyo, Japan). Raman scattering spectra of powders were recorded at room temperature from a Raman spectrometer (Model T64000, Jobin-Yvon, Paris, France) under backscattering geometry. Excitation was taken as the 488 nm line of $Ar^+$ laser with 50 mW output power.

## 3. Results and discussion

It has been reported in many papers, that the observed O–T PPT seem to be inherited from the $KNbO_3$ system.[3,19,20] The effect of $LiNbO_3$ doping shifts the phase transition temperatures without altering the order of polymorphic transitions.[21] So, like $KNbO_3$ powders, the size effect on nanoscale LNKN powders would show a phase transition rather than a relative contents change of *orthorhombic and tetragonal* phase.

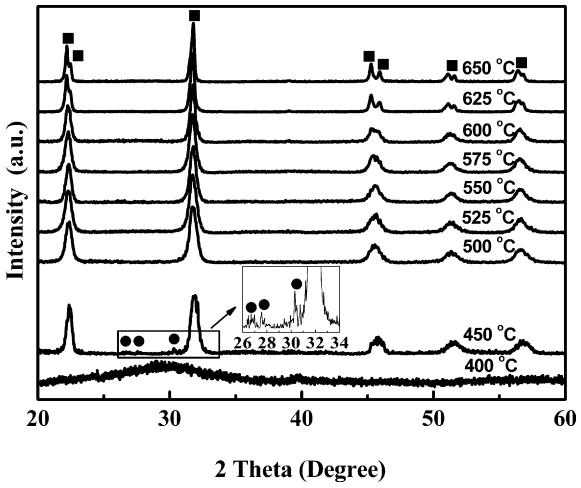


Fig. 1. XRD patterns of LNKN gel powders annealed at various temperatures: ■, perovskite; ●, impurity phases.

The crystallization process of the LNKN gels annealed at various temperatures was monitored, as shown in Fig. 1. The powders calcinated below 400 °C exhibit the typical amorphous pattern, showing a broad peak around 30°. When the annealing temperature reaches 450 °C, the characteristic diffraction peaks of LNKN crystals begin to appear. However, there still exist some impurity phases, as marked with "●". With further increasing temperature to 500 °C and above, only pure LNKN perovskite phase can be observed and there was no evidence of second phase.

It is well known that both the small grain size and microstrain can cause the distinct broadening of diffraction lines. According to this, based on Eq. (1), the average grain size of LNKN powder with different annealing temperature was refined using Topas 2P software, and the results and errors are shown in Fig. 2. The inset in Fig. 2 shows the variation of microstrain with dif-

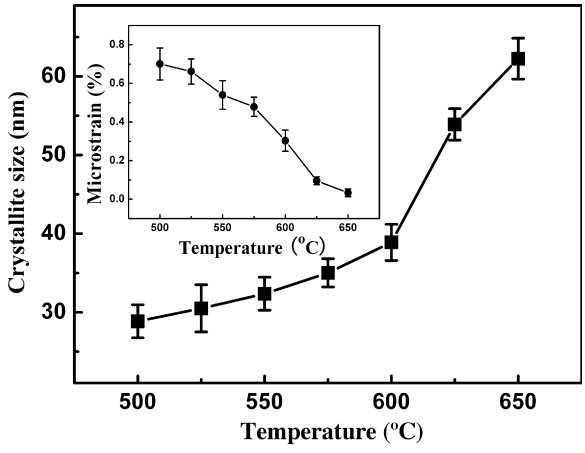


Fig. 2. Variation of the grain size with the annealing temperature. Inset: variation of the microstrain with the annealing temperature.

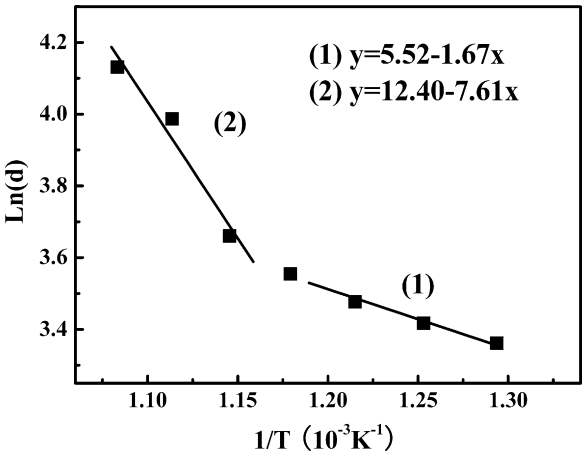


Fig. 3. Relation of the grain size on a log scale with the inverse of the calcined temperature.

ferent annealing temperature, resulting also from the refinement by Topas 2P. It can be observed that the increase of annealing temperature facilitates the depressing of microstrain and coarsening of the nano powders. In the studied temperature region, with the *increase* of annealing temperature the microstrain of LNKN powder has decreased from 0.70% at 500 °C to 0.03% at 650 °C, while the average grain size has increased from 28.9 nm to 62.2 nm. In our experiment, below 575 °C, the crystalline grain grows up gradually with the increase of annealing temperature; however, the growth rate becomes increscent when the temperature further increases above 575 °C. It is known that the growth of grains can be described by the following equation[22]:

$$d = d_0 \exp\left(\frac{-E_a}{k_B T}\right) \quad (2)$$

where $d$ is the grain size, $d_0$ a constant, $E_a$ the activation energy, and $k_B$ the Boltzmann constant. The activation energy can be calculated from Eq. (2) using the data in Fig. 2. Fig. 3 shows the grain size on a log scale with the inverse of the annealing temperature. It can be clearly seen that the growth process of grains has been divided into two stages. Through the linear regression in curves (1) and (2), the activation energy of the LNKN sample can be obtained, and the results show that $E_{a1}$ is 1.44 eV when the annealing temperature is below 575 °C, while $E_{a2}$ is 6.56 eV when the temperature is over 575 °C, respectively. Generally, it should be noted that the growth of grains under different annealing temperatures has mainly two stages, the first stage includes the removal of internal stress and the interface structure relaxation at lower temperature; the second is mainly the growth of grains at high temperature. The energy for the interface structure relaxation is usually smaller than that for the growth of the grains, so the grains grow slowly at low annealing temperature and grow rapidly at high annealing temperature.[22]

Fig. 4 shows a representative TEM image of LNKN annealed at 500 °C. It can be observed that the nanoscale LNKN particles are nearly square, and the soft agglomeration of particles is well dispersed. The average grain size is about 30 nm, which agrees with the result determined by XRD well. The inset of SAED

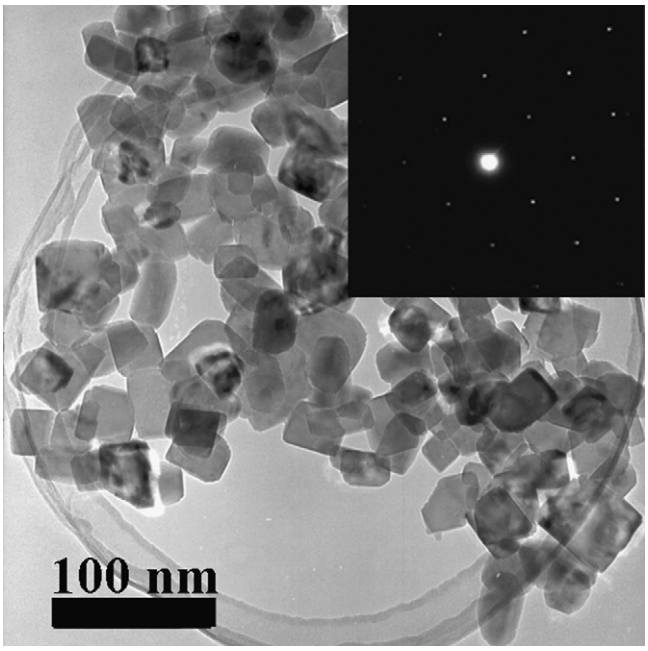


Fig. 4. TEM image of LNKN annealed at 500 °C. Inset: the SAED pattern of a typical LNKN particle.

pattern recorded from an individual particle confirms that the nanoscale LNKN is single-crystal structure.

Fig. 5 shows the fine scanning XRD patterns in $2\theta$ range of 43.5°–47.5° of LNKN powders with different grain sizes and Lorentz curve simulation. In addition to the decrease of the grain size, it can be seen in Fig. 5 that the crystal structure of the specimens is modified profoundly (from orthorhombic to tetragonal), as revealed by the splitting change and intensity ratio of the (2 0 2) and (0 2 0) peaks. The LNKN powders with grain size of 35.0 nm can be seen as an intermediate state of O–T phase transition. The structure illustration for

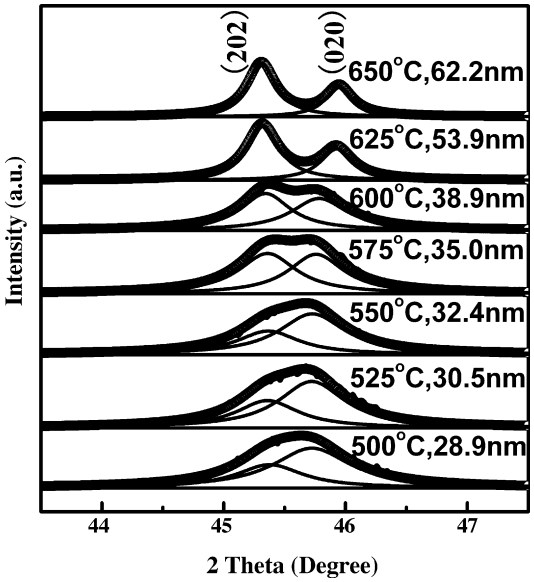


Fig. 5. Fine scanning XRD patterns in $2\theta$ range of 43.5°–47.5° of LNKN powders with different grain sizes and Lorentz curve simulation.

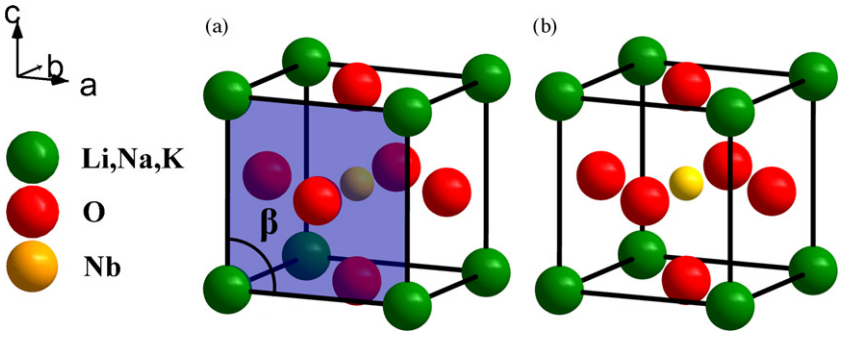


Fig. 6. The structure illustration for (a) orthorhombic and (b) tetragonal phase of LNKN. The perovskite type $ABO_3$ subcell of orthorhombic phase LNKN possesses monoclinic symmetry, with lattice parameters $a_m = c_m > b_m$ while $b_m$ axis is perpendicular to $a_m c_m$ plane and angle $\beta$ is a little more than 90°. While the tetragonal phase LNKN possesses tetragonal symmetry with lattice parameters $a_t = b_t < c_t$. (For interpretation of the references to color, the reader is referred to the web version of the article.)

orthorhombic and tetragonal phase of LNKN is shown in Fig. 6. It is known that the perovskite type $ABO_3$ subcell of orthorhombic phase LNKN possesses monoclinic symmetry, as shown in Fig. 6(a), with lattice parameters $a_m = c_m > b_m$ while $b_m$ axis is perpendicular to $a_m c_m$ plane and angle $\beta$ is a little more than 90°.[23–25] The perovskite type $ABO_3$ subcell of tetragonal phase LNKN is shown in Fig. 6(b), and possesses tetragonal symmetry with lattice parameters $a_t = b_t < c_t$.

For orthorhombic phase LNKN powders, firstly, according to the standard card of orthorhombic $KNbO_3$ (JCPDS No. 71-2171), the lattice constants $a_o, b_o, c_o$ were calculated by the XRD data from Fig. 1. To accurately determine the lattice constants, many well-resolved diffraction peaks, such as (1 0 1), (0 1 0), (0 0 2), (2 0 0), (1 1 1), (2 0 2), and (0 2 0), were used in the least-squares calculations. Then $a_m$, $b_m$, $c_m$ can be calculated by the following equations:

$$a_m = c_m = \frac{1}{2}\sqrt{a_o^2 + c_o^2} \tag{3}$$

$$b_m = b_o \tag{4}$$

$$\beta = 180 - 2\text{atan}\left(\frac{a_o}{c_o}\right) \tag{5}$$

The lattice parameters of tetragonal phase LNKN were calculated according to the standard card of tetragonal $KNbO_3$ (JCPDS No. 71-0945), in which (0 0 1), (1 0 0), (1 0 1), (1 1 0), (0 0 2) and (2 0 0) were used. Fig. 7 shows the variation of the lattice constants as a function of grain size at room temperature. It is clearly shown that the structure of the solid solution transforms from orthorhombic to tetragonal symmetry with the decrease of the grain size, and the critical size of the O–T phase transition for LNKN is around 35 nm, which is shown as a shadow region in Fig. 7. This result indicated that the grain structure of LNKN powder was strongly influenced by the grain size and the phase structure changes from orthorhombic to tetragonal at around 35 nm. So, it can be concluded that the so-called O–T phase transition is not only affected by composition and temperature, but also show strong size dependence. Moreover, the $c_t/a_t$ ratio of the LNKN powders with average grain size of 28.9 nm is 1.008. It can be expected that, if the high-symmetry cubic structure exists, it would occur at the grain size less than 28.9 nm. In order to further confirm the tetragonal-cubic phase transitional behavior, further experiment is needed.

Raman spectroscopy is one of the powerful tools available to analyze the changes of phase structure due to its sensitivity even to very small distortions of the crystal lattice. Recently, researches on Raman spectra of KNN-based systems indicate that vibrations of $NbO_6$ octahedron are sensitive to the occurrence of phase transitions.[8,26,27] In this work, the Raman spectra of LNKN powders with different grain sizes are shown in Fig. 8. Internal vibration modes of the $NbO_6$ octahedra appear in a wide range from 100 to 1000 $cm^{-1}$. Regarding the equilateral octahedron symmetry ($O_h$) of a free $NbO_6$, $\nu_1$ mode near 610 $cm^{-1}$ represents a double-degenerate symmetric O-Nb-O stretching vibration, and $\nu_5$ mode near 260 $cm^{-1}$ represents a triply degenerate symmetric O-Nb-O bending vibration. The Fig. 9 shows variation of the *wavenumber* of $\nu_1$ mode as a function of grain size at room temperature. With the decrease of grain size from 62.2 to 28.9 nm, the *wavenumber* of the $\nu_1$ mode decreases obviously from 612 to 605 $cm^{-1}$. The same change trend is observed in the $\nu_5$ mode as well. These changes denote the grain size induced the phase transition from orthorhombic to tetragonal, which is similar to the observation in thermodynamics phase transition on NKN based systems.[27] Furthermore, the occurrence of $\nu_1 + \nu_5$ at 860 $cm^{-1}$ can be attributed to the asymmetric

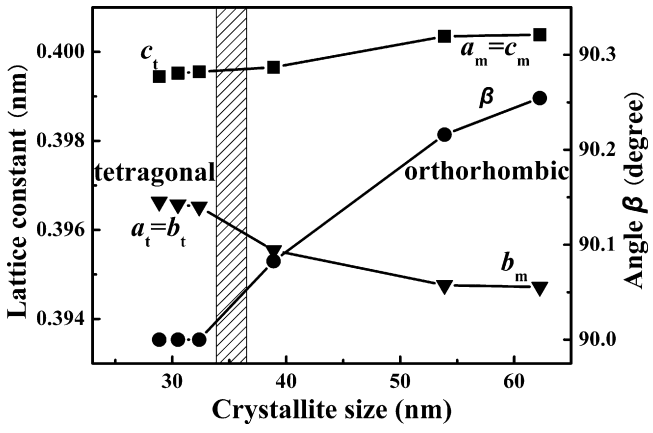


Fig. 7. Variation of the lattice constants as a function of grain size at room temperature.

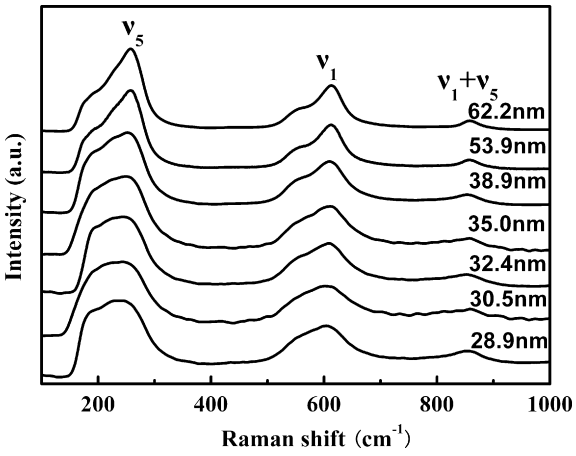


Fig. 8. Raman spectra of LNKN powders with different grain sizes.

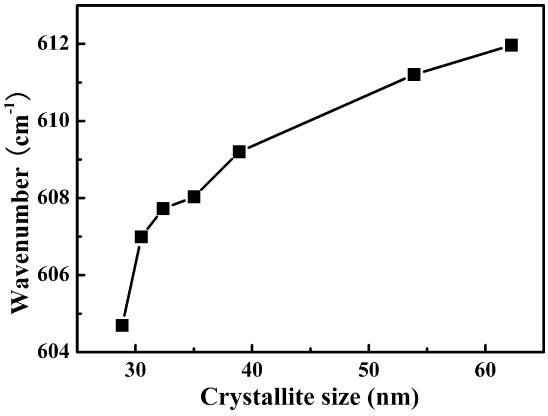


Fig. 9. Variation of the *wavenumber* of $\nu_1$ mode as a function of grain size at room temperature.

phase structure.[8] That is to say, though the grain size decreases to about 30 nm, the phase structure of LNKN powders is still not changed to cubic symmetry due to the existence of weak mode of $\nu_1 + \nu_5$, which agrees well with the evidence of the refinement of the lattice constants in the former XRD analysis.

It is known that in $ABO_3$ perovskite ferroelectrics systems, the center B cation in $BO_6$ octahedra has the lowest unoccupied *d*-states. This allows for *d*-hybridization with the coordinated oxygen that softens the B-O repulsion. With the decrease of LNKN grain size, the ratio of surface atoms increased. Therefore, the additional microstrain (see the inset figure of Fig. 2) induced by small grain size can strengthen the short-range forces, which enhance the hybridization between the Nb and its coordinated oxygen.[28] Accordingly, the binding strength of Nb-O decreased, resulting in the softening of Raman modes and phase transition from orthorhombic to tetragonal.

## 4. Conclusions

Nanoscale LNKN powders with pure perovskite structure have been synthesized successfully by a novel sol–gel process. In the studied annealing temperature region, the average grain size of LNKN powder has increased from about 30 nm at 500 °C to 60 nm at 650 °C. The size dependences of the crystal structure and Raman spectra have been investigated, which revealed that the critical size of the phase transition from orthorhombic to tetragonal for the LNKN nano powders is around 35 nm. The additional microstrain induced by small grain size can give a reason for the phase transition of the LNKN nano powders. Because it has been approved that niobates get super piezoelectric properties in O–T transition region, the results in this paper could suggest a critical size for the application of LNKN in nano piezoelectric devices.

## Acknowledgements

This work was funded by the National Natural Science Foundation of China (NSFC) (Grant no. 60601020), the Natural Science Foundation of Beijing (Grant no. 4072006), the Project of New Star of Science and Technology of Beijing (Grant no. 2007A014), and the Science and Technology Development Project of Beijing Education Committee (Grant no. KM200810005012).

## References

1. Guo, R., Cross, L. E., Park, S. E., Noheda, B., Cox, D. E. and Shirane, G., Origin of the high piezoelectric response in $PbZr_{1-x}Ti_xO_3$. *Phys. Rev. Lett.*, 2000, **84**, 5423–5426.
2. Noheda, B., Gonzalo, J. A., Cross, L. E., Guo, R., Park, S. E., Cox, D. E. *et al.*, Tetragonal-to-monoclinic phase transition in a ferroelectric perovskite: the structure of $PbZr_{0.52}Ti_{0.48}O_3$. *Phys. Rev. B*, 2000, **61**, 8687–8695.
3. Shrout, T. R. and Zhang, S. J., Lead-free piezoelectric ceramics: alternatives for PZT? *J. Electroceram.*, 2007, **19**, 111–124.
4. Chang, Y. F., Yang, Z. P., Ma, D. F., Liu, Z. H. and Wang, Z. L., Phase transitional behavior, microstructure, and electrical properties in Ta-modified $[(K_{0.458}Na_{0.542})_{(0.96)}Li_{0.04}]NbO_3$ lead-free piezoelectric ceramics. *J. Appl. Phys.*, 2008, **104**, 024109-1–024109-8.
5. Wang, K., Li, J. F. and Liu, N., Piezoelectric properties of low-temperature sintered Li-modified (Na, K)$NbO_3$ lead-free ceramics. *Appl. Phys. Lett.*, 2008, **93**, 092904-1–092904-3.
6. Saito, Y., Takao, H., Tani, T., Nonoyama, T., Takatori, K., Homma, T. *et al.*, Lead-free piezoceramics. *Nature*, 2004, **432**, 84–87.
7. Guo, Y. P., Kakimoto, K. and Ohsato, H., Phase transitional behavior and piezoelectric properties of $(Na_{0.5}K_{0.5})NbO_3$-$LiNbO_3$ ceramics. *Appl. Phys. Lett.*, 2004, **85**, 4121–4123.
8. Klein, N., Hollenstein, E., Damjanovic, D., Trodahl, H. J., Setter, N. and Kuball, M., A study of the phase diagram of (K, Na, Li)$NbO_3$ determined by dielectric and piezoelectric measurements, and Raman spectroscopy. *J. Appl. Phys.*, 2007, **102**, 014112-1–014112-8.
9. Kinoshita, K. and Yamaji, A., Grain-size effects on dielectric properties in barium titanate ceramics. *J. Appl. Phys.*, 1976, **47**, 371–373.
10. Ishikawa, K., Yoshikawa, K. and Okada, N., Size effect on the ferroelectric phase transition in $PbTiO_3$ ultrafine particles. *Phys. Rev. B*, 1988, **37**, 5852–5855.
11. Smith, M. B., Page, K., Siegrist, T., Redmond, P. L., Walter, E. C., Seshadri, R. *et al.*, Crystal structure and the paraelectric-to-ferroelectric phase transition of nanoscale $BaTiO_3$. *J. Am. Chem. Soc.*, 2008, **130**, 6955–6963.
12. Zhou, Q. F., Chan, H. L. W., Zhang, Q. Q. and Choy, C. L., Raman spectra and structural phase transition in nanocrystalline lead lanthanum titanate. *J. Appl. Phys.*, 2001, **89**, 8121–8126.
13. Shiratori, Y., Magrez, A. and Pithan, C., Phase transformation of $KNaNb_2O_6$ induced by size effect. *Chem. Phys. Lett.*, 2004, **391**, 288–292.
14. Predoană, L., Barău, A., Zaharescu, M., Vassilchina, H., Velinova, N., Banov, B. *et al.*, Electrochemical properties of the $LiCoO_2$ powder obtained by sol-gel method. *J. Eur. Ceram. Soc.*, 2007, **27**, 1137–1142.

15. Linardos, S., Zhang, Q. and Alcock, J. R., Preparation of sub-micron PZT particles with the sol-gel technique. *J. Eur. Ceram. Soc.*, 2006, **26**, 117–123.
16. Krebs, J. K. and Happek, U., Optical spectroscopy of trivalent chromium in sol-gel lithium niobate. *Appl. Phys. Lett.*, 2005, **87**, 251910-1–251910-3.
17. Wang, C., Hou, Y. D., Ge, H. Y., Zhu, M. K., Wang, H. and Yan, H., Sol-gel synthesis and characterization of lead-free LNKN nanocrystalline powder. *J. Cryst. Growth*, 2008, **310**, 4635–4639.
18. Birks, L. S. and Friedman, H., Particle size determination from x-ray line broadening. *J. Appl. Phys.*, 1946, **17**, 687–692.
19. Triebwasser, S., Study of ferroelectric transitions of solid-solution single crystals of $KNbO_3$-$KTaO_3$. *Phys. Rev.*, 1959, **114**, 63–70.
20. Zhang, S. J., Xia, R., Shrout, T. R., Zang, G. and Wang, J., Piezoelectric properties in perovskite $0.948(K_{0.5}Na_{0.5})NbO_3$-$0.052LiSbO_3$ lead-free ceramics. *J. Appl. Phys.*, 2006, **100**, 104108-1–104108-6.
21. Akdoğan, E. K., Kerman, K., Abazari, M. and Safari, A., Origin of high piezoelectric activity in ferroelectric $K_{0.44}Na_{0.52}Li_{0.04}Nb_{0.84}Ta_{0.1}Sb_{0.06}O_3$ ceramics. *Appl. Phys. Lett.*, 2008, **92**, 112908-1–112908-3.
22. Ishikawa, K., Okada, N., Takada, K., Nomura, T. and Hagino, M., Crystallization and growth process of lead titanate fine particles from alkoxide-prepared powders. *Jpn. J. Appl. Phys.*, 1994, **33**, 3495–3499.
23. Shirane, G., Newnham, R. and Pepinsky, R., Dielectric properties and phase transitions of $NaNbO_3$ and $(Na,K)NbO_3$. *Phys. Rev.*, 1954, **96**, 581–588.
24. Tennery, V. J. and Hang, K. W., Thermal and x-ray diffraction studies of the $NaNbO_3$-$KNbO_3$ System. *J. Appl. Phys.*, 1968, **39**, 4749–4753.
25. Wang, K. and Li, J. F., Analysis of crystallographic evolution in $(Na,K)NbO_3$-based lead-free piezoceramics by x-ray diffraction. *Appl. Phys. Lett.*, 2007, **91**, 262902-1–262902-3.
26. Kakimoto, K., Akao, K., Guo, Y. P. and Ohsato, H., Raman scattering study of piezoelectric $(Na_{0.5}K_{0.5})NbO_3$-$LiNbO_3$ ceramics. *Jpn. J. Appl. Phys.*, 2005, **44**, 7064–7067.
27. Dai, Y. J., Zhang, X. W. and Zhou, G. Y., Phase transitional behavior in $K_{0.5}Na_{0.5}NbO_3$–$LiTaO_3$ ceramics. *Appl. Phys. Lett.*, 2007, **90**, 262903-1–262903-3.
28. Meng, J. F., Katiyar, R. S. and Zou, G. T., Grain size effect on ferroelectric phase transition in $Pb_{1-x}Ba_xTiO_3$ ceramics. *J. Phys. Chem. Solids*, 1998, **59**, 1161–1167.